

Geophysical Research Letters®

RESEARCH LETTER

10.1029/2022GL098469

Key Points:

- Subauroral ion drifts (SAID) are associated with higher plasma sheet electron fluxes and sharper flux gradients just outside the velocity peak
- Strong electron injection is the primary condition for creating SAID. SAID do not require strong ring current ions
- Local plasma structures are more important for subauroral polarization streams (SAPS)/SAID than IMF and global magnetospheric conditions

Supporting Information:

Supporting Information may be found in the online version of this article.

Correspondence to:

Y. Nishimura,
ynishimura11@gmail.com

Citation:

Nishimura, Y., Hussein, A., Erickson, P. J., Gallardo-Lacourt, B., & Angelopoulos, V. (2022). Statistical study of magnetospheric conditions for SAPS and SAID. *Geophysical Research Letters*, 49, e2022GL098469. <https://doi.org/10.1029/2022GL098469>

Received 8 MAR 2022

Accepted 21 APR 2022

Author Contributions:

Conceptualization: Y. Nishimura, P. J. Erickson, B. Gallardo-Lacourt
Data curation: V. Angelopoulos
Formal analysis: Y. Nishimura, A. Hussein
Funding acquisition: Y. Nishimura, V. Angelopoulos
Investigation: Y. Nishimura, A. Hussein
Methodology: Y. Nishimura, A. Hussein, P. J. Erickson
Project Administration: Y. Nishimura
Resources: Y. Nishimura
Software: Y. Nishimura, A. Hussein
Supervision: Y. Nishimura
Validation: Y. Nishimura
Visualization: Y. Nishimura
Writing – original draft: Y. Nishimura
Writing – review & editing: P. J. Erickson

© 2022. American Geophysical Union.
All Rights Reserved.

Statistical Study of Magnetospheric Conditions for SAPS and SAID

Y. Nishimura¹ , A. Hussein¹ , P. J. Erickson² , B. Gallardo-Lacourt^{3,4} , and V. Angelopoulos⁵ 

¹Department of Electrical and Computer Engineering and Center for Space Physics, Boston University, Boston, MA, USA

²Haystack Observatory, Massachusetts Institute of Technology, Westford, MA, USA, ³NASA Goddard Space Flight Center, Greenbelt, MD, USA, ⁴Universities Space Research Association, Columbia, MD, USA, ⁵Department of Earth, Planetary, and Space Sciences, University of California, Los Angeles, CA, USA

Abstract Inner-magnetospheric conditions for subauroral polarization streams (SAPS) and subauroral ion drifts (SAID) have been investigated statistically using Time History of Events and Macroscale Interactions during Substorms and RBSP observations. We found that plasma sheet electron fluxes at its earthward edge are larger for SAID than SAPS. The ring current ion flux for SAID formed a local maximum near SAID, but the ion flux for SAID was not necessarily larger than for SAPS. The median potential drop across SAID and SAPS is nearly the same, but the potential drop for intense SAID is substantially larger than that for SAPS. The plasmapause is sharper and electromagnetic waves were more intense for SAID. The SAID velocity peak does not strongly correlate with solar wind or geomagnetic indices. These results indicate that local plasma structures are more important for SAPS/SAID velocity characteristics as compared to global magnetospheric conditions.

Plain Language Summary The mid-latitude ionosphere and inner magnetosphere have fast plasma streams. Intense plasma streams have recently gained attention because they are associated with the STEVE phenomenon. However, it has not been understood what magnetospheric processes determine the strength and width of the fast plasma streams. We conducted a statistical study of plasma streams using >400 events from NASA's Time History of Events and Macroscale Interactions during Substorms and Van Allen Probes satellite observations to firmly address this question. We found that faster plasma streams are associated with higher electron fluxes than subauroral polarization streams. Ion fluxes for faster plasma streams are more localized but the magnitude is not enhanced. The peak velocity does not correlate with solar wind or geomagnetic conditions. We suggest that local plasma structures are more important for velocity characteristics of fast plasma streams compared to solar wind or global magnetospheric conditions.

1. Introduction

Plasma convection in the subauroral pre-midnight ionosphere is often characterized by fast sunward flow channels of a few degree widths called subauroral polarization streams (SAPS) (Foster & Burke, 2002). SAPS are an important feature in inner magnetosphere-ionosphere coupling, where field-aligned currents flow downward from the ring current to the subauroral ionosphere and return to the magnetosphere as upward currents to the electron plasma sheet (Anderson et al., 1993). The conductance in the subauroral ionosphere is low (mid-latitude trough), and a strong electric field (i.e., SAPS) is required to close the current. SAPS typically occur during geomagnetically disturbed times (Foster & Vo, 2002; Wang et al., 2008), because injection of energetic particles to the inner magnetosphere strengthens this current system.

SAPS occasionally exhibit latitudinally narrow velocity spikes (>1 km/s and ~1° width) known as subauroral ion drifts (SAID) (Foster & Burke, 2002; Galperin, 2002). SAID have an impact on ionospheric composition changes (Anderson et al., 1991), and intense SAID are involved in STEVE (MacDonald et al., 2018; Nishimura et al., 2019). Thus understanding magnetospheric driving conditions for SAID has a unique impact on ionospheric dynamics. However, SAPS and SAID have similar occurrence characteristics, and little is known about what magnetospheric conditions determine whether SAID develop or not. Here for convenience, we refer to SAPS as weaker flows (250–1,000 m/s) excluding SAID (>1 km/s) in the ionosphere. While SAID are included in the original definition of SAPS (Foster & Burke, 2002), we separate SAPS and SAID here to exclusively discuss magnetospheric conditions of SAPS and SAID.

Both SAPS and SAID most commonly occur in pre-midnight sectors (Foster & Vo, 2002; He et al., 2014; Karlsson et al., 1998). Both SAPS and SAID are located between the equatorward edges of electron and ion precipitation (Mishin & Puhl-Quinn, 2007; Nishimura et al., 2008; Yeh et al., 1991). Although SAID also tend to occur during geomagnetically disturbed times (Anderson et al., 1993), SAID do not necessarily favor stronger geomagnetic activity but can also occur at weak geomagnetic activity (Karlsson et al., 1998; Wang et al., 2008).

Recent studies using a small set of events have shown that SAID are associated with both a sharper gradient of plasma sheet electron flux and a narrower gap between the equatorward boundaries of ring current ions and precipitating plasma sheet electrons, as compared to SAPS events (Nishimura, Donovan, et al., 2020; Nishimura, Yang, et al., 2020). This work led to the inference that stronger electron injection transports more electrons earthward and reduces the separation between the plasma sheet electrons and ring current ions. However, this inference has not been statistically demonstrated. It is also possible that larger fluxes of ring current ions may result in larger velocity, because SAPS and SAID structures are closely associated with the dynamics of ring current ion populations (Mishin & Puhl-Quinn, 2007; Yeh et al., 1991). Short-circuiting of currents at the plasmapause has also been suggested as a mechanism for SAID (Mishin & Puhl-Quinn, 2007). These potential mechanisms should be examined statistically in order to identify what magnetospheric structures determine the strength and width of the flow channel. To date, however, although many case studies of SAPS and SAID in the inner magnetosphere have been performed, statistical investigations of SAPS and SAID in the inner magnetosphere have been very limited (Lejosne & Mozer, 2017).

We conduct a statistical study of SAPS and SAID in the inner magnetosphere to identify how SAPS and SAID are related to plasma boundaries and waves. We show that local ion and electron fluxes for SAID and SAPS have statistically significant differences. Furthermore, peak ion fluxes do not correlate with the flow velocity, and the electric field is not fully shielded at the plasmapause.

2. Data and Method

The SAID and SAPS events were identified using the Time History of Events and Macroscale Interactions during Substorms (THEMIS) A through E and Van Allen Probes (RBSP) A and B satellite datasets acquired in the inner magnetosphere in the dusk-to-midnight sector (16–24 hr MLT within $6.6 R_E$). This region covers much of SAPS and SAID occurrence (Foster & Vo, 2002; He et al., 2014). The event survey used data from THEMIS-A, D and E in 2008–2020, THEMIS-B and C in 2008–2009, and RBSP-A and B in 2013–2018.

SAID were identified as channels of westward plasma drift with >10 km/s speed and $<0.2 R_E$ radial full width at half maximum (FWHM) for individual events. The velocity threshold was chosen by considering that SAID in the ionosphere are defined as >1 km/s westward velocity and typically have $<1^\circ$ latitudinal widths (Anderson et al., 1991). The 1 km/s speed and 1° latitudinal width at 60° MLAT (near the highest statistical occurrence of SAPS and SAID (Foster & Vo, 2002; He et al., 2014)) magnetically maps to ~ 10 km/s speed and $\sim 0.2 R_E$ width at $\sim 4 R_E$ in the magnetosphere. To distinguish SAID from other types of velocity enhancements (e.g., large-scale convection and ULF waves), velocity enhancements were further restricted to locations just earthward of the electron plasma sheet and within the ring current ions. The velocity enhancement was also required to be an isolated spike (typical SAID) or two adjacent spikes (double SAID) (He et al., 2016). This criterion excluded velocity enhancements with more than two peaks as being likely ULF waves or rapid temporal variation of convection. Events with sudden magnetic field jumps were also removed because they likely involve temporal variations such as particle injections and interplanetary shocks. After these filters were applied, we identified 202 SAID events that satisfy these criteria (Table S1 in Supporting Information S1).

SAPS were identified using the same method, except that the westward velocity peak requirement was 3–10 km/s and the radial width was allowed to be as broad as the separation between the earthward boundaries of the ring current ions and plasma sheet electrons. The lower 3 km/s velocity limit considers that SAPS in the ionosphere are often defined as >250 m/s westward velocity (Foster & Vo, 2002). The upper 10 km/s limit was given to exclude SAID. Note that this study is conservative and does not investigate SAPS with >10 km/s velocity enhancements and $>0.2 R_E$ FWHM, because such events often contain narrow velocity spikes that resemble SAID and it is difficult to classify them as SAPS or SAID. Applying these criteria resulted in 201 SAPS events (Table S2 in Supporting Information S1).

Note that SAPS observations are more subject to temporal variations, and there may be more events than we have cataloged. SAID observations can be regarded as measuring the spatial extent of the velocity field because a satellite crossing of SAID only takes a few minutes (much shorter than the lifetime of SAID, ~ 30 min (Anderson et al., 1991; Lejosne & Mozer, 2017)). In contrast, SAPS crossings could take tens of minutes and observations are more likely disturbed by other phenomena. SAPS are also weaker than SAID and are easily obscured by convection variations or ULF waves.

The merged velocity moment from the electrostatic analyzer (ESA) and solid state detector (SST) onboard THEMIS provided the westward velocity as weighted average of velocity moments (Angelopoulos et al., 2019). Due to the energy gap, density moments are generally underestimated, but velocity moments can find velocity as long as the bulk of distribution function is measured. For RBSP, the electric field from the EFW instrument was used to obtain the westward velocity. Validity of using electric field measurements for SAPS was demonstrated by Anderson et al. (2001). The spin-axis electric field was calculated using $E \cdot B = 0$ (Nishimura et al., 2006, 2022; Ali et al., 2016). Events where the magnetic field is $<5^\circ$ angle from the spin plane were not used in this work. The cold plasma density for THEMIS was obtained from the spacecraft potential (Nishimura et al., 2013). The cold plasma density for RBSP was obtained from the upper-hybrid frequency (RBSP) (Kurth et al., 2015), or from the spacecraft potential (Thaller et al., 2015) when the density from the upper-hybrid frequency was not available. Intensities of low-frequency electric and magnetic field waves were obtained from the filter-bank dataset from THEMIS. We did not use wave observations from RBSP's EMFISIS instrument because it was difficult to merge them with the THEMIS dataset with proper cross-calibration. Data from the electric field instruments were removed when the satellites were located in the Earth's shadow. Wave electric field data were also removed when the booms were in the satellite shadow.

Figure 1 shows an example of a selected SAID (left) and SAPS (right) event. Both events were detected by THEMIS at similar locations ($\sim 3.8 R_E$ in the pre-midnight sector), UT (1–2 hr) and season (April). Figure 1a shows an isolated westward velocity enhancement reaching 36 km/s with $<0.1 R_E$ FWHM. This velocity peak was located at the earthward edge of the electron plasma sheet (Figure 1d) within the enhanced ring current ion population (Figure 1e). This velocity enhancement was thus identified as SAID. The outer edge of the velocity enhancement was within the gradient of the electron flux. The low-energy ions shown in the SAID are cold ions whose bulk flow energy reached a few tens of eV (Lee & Angelopoulos, 2014), and validate that the velocity enhancement was present. Additionally, the earthward boundary of SAID was collocated with a sharp gradient of the ring current ion flux, and the SAID flow channel was confined between the sharp gradients of the ring current ions and plasma sheet electrons. The SAID event was also associated with an earthward gradient of ΔB_z (Figure 1b; a quiet-time background magnetic field using T01 (Tsyganenko, 2002) was subtracted), sharp plasmapause (Figure 1c), and broadband electromagnetic waves (Figures 1f and 1g). These features are consistent with past observations (for example, Mishin et al., 2010; Nishimura et al., 2019).

Figure 1h shows a different isolated, weaker, and broader velocity enhancement. The velocity peak was also found at the earthward edge of the electron plasma sheet within the ring current ions (Figures 1k and 1l). Thus it was identified as a SAPS flow. The outer edge of SAPS had weak electron fluxes at the gradient of the electron plasma sheet flux. For this encounter, cold ions were seen at the lowest energy channels near the peak of the SAPS velocity, supporting the existence of the enhanced velocity again due to bulk flow energy. The inner edge of SAPS was in the region of the ring current ion flux gradient. In aggregate, therefore, the SAPS flow was also confined between the gradients of the ring current ion and plasma sheet electron fluxes.

However, there are notable differences between the two events in Figure 1. Specifically, the ring current ions and plasma sheet electrons for the SAPS event were more radially separated, and both gradients were smaller. The fluxes and energy of the plasma sheet electrons for SAPS were also lower, and the electron fluxes were more energy-dispersed than those for SAID. The density gradient at the plasmapause was more gradual. There was no substantial enhancement of the electromagnetic waves in the measured frequency range (Figures 1m and 1n). The ring current ion fluxes were also lower, but we later show in Section 3 that the ion fluxes are typically comparable.

To characterize the ring current ions and plasma sheet electrons, we defined them as regions of $>1.5 \cdot 10^{11}$ [eV/cm² s] total energy fluxes at <50 keV (ions) and $>2 \cdot 10^{12}$ [eV/cm² s] at <30 keV (electrons). Those numbers were chosen empirically as typical values at the earthward boundaries of the ring current ions and plasma sheet

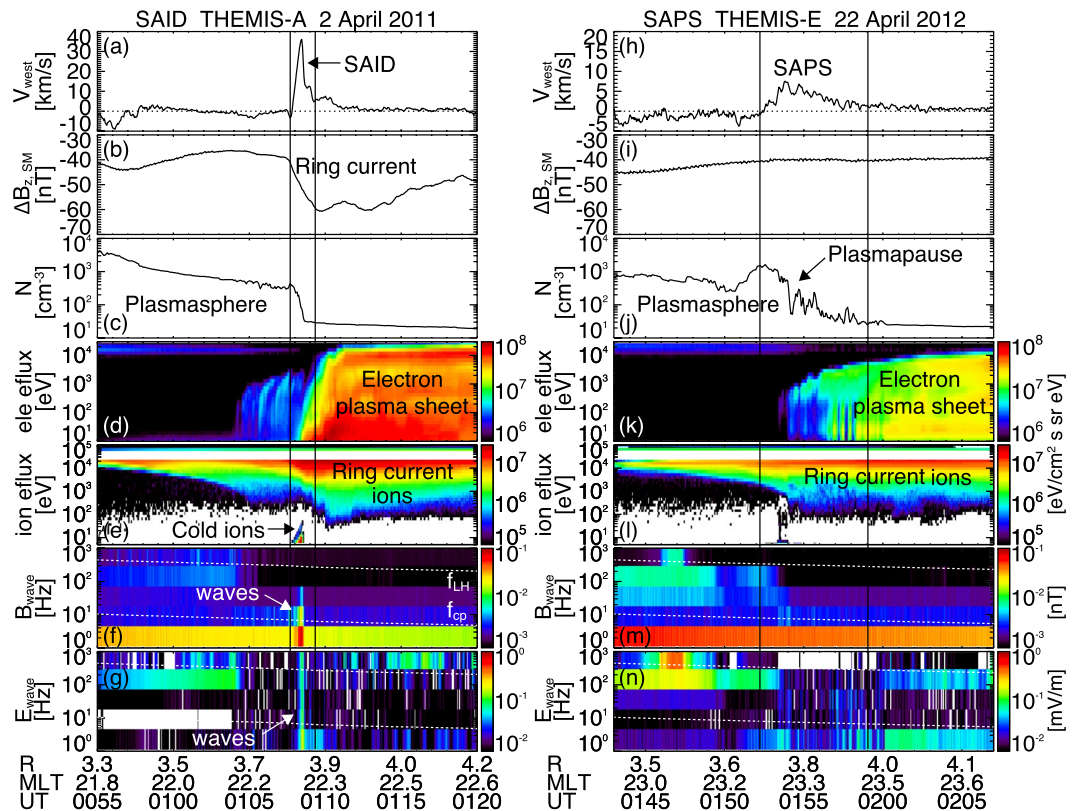


Figure 1. Example (left) subauroral ion drifts (SAID) and (right) subauroral polarization streams (SAPS) events. (a and h) Westward velocity, (b and i) ΔB_z , (c and j) total plasma density, (d and k) omni-directional electron energy flux, (e and l) omni-directional ion energy flux, (f and m) magnetic field wave spectrogram, and (g and n) electric field wave spectrogram. The dashed lines in the bottom two panels show the lower-hybrid and proton gyro frequencies.

electrons. For THEMIS, the energy gap between the ESA and SST instruments was interpolated to obtain the total ion flux up to 50 keV. Finally, wave electric and magnetic fields were integrated below the lower-hybrid frequency to cover kinetic Alfvén waves and lower-hybrid waves (typically below the 192 Hz bin).

3. Statistical Study

Using the Table S1 and S2 in Supporting Information S1 events, we performed a superposed epoch analysis of the SAID and SAPS events as shown in Figures 2 and 3. The epoch time is UT of the peak westward velocity. The median represents the typical radial distribution of the parameters within $1 R_E$ from the velocity peaks and the quartiles indicate their variance. The 10 and 90 percentiles depict behavior of extreme events. Figures 2a and 2b confirm that the SAID are confined within a fraction of R_E , while the SAPS velocity spreads over wider radial distances.

Both SAID and SAPS are located just earthward of the electron plasma sheet, and the electron flux gradient for SAID was steeper than the gradient for SAPS (Figures 2c and 2d). All five percentiles consistently show that the electron flux for SAID at $\Delta r = 0.1 R_E$ was about 50% larger than that for SAPS. In contrast, the electron flux at $\Delta r = 1 R_E$ in the two panels was comparable, indicating that electron plasma sheet conditions at higher L -shells do not have major differences, but that electrons are consistently injected deeper into the inner magnetosphere for SAID events. This result extends the finding from a small number of events (Nishimura, Donovan, et al., 2020; Nishimura, Yang, et al., 2020) to a statistically significant and generally true conclusion.

Results also show that SAID are located near the peak of the ring current ion flux, and the ion flux at $\Delta r > 0$ is lower than that for SAPS (Figures 2e and 2f). The ring current flux for SAPS is nearly constant at $\Delta r > 0$ and SAPS are located at the outward gradient of the ion flux. The ion flux at $\Delta r < 0$ has an outward gradient for

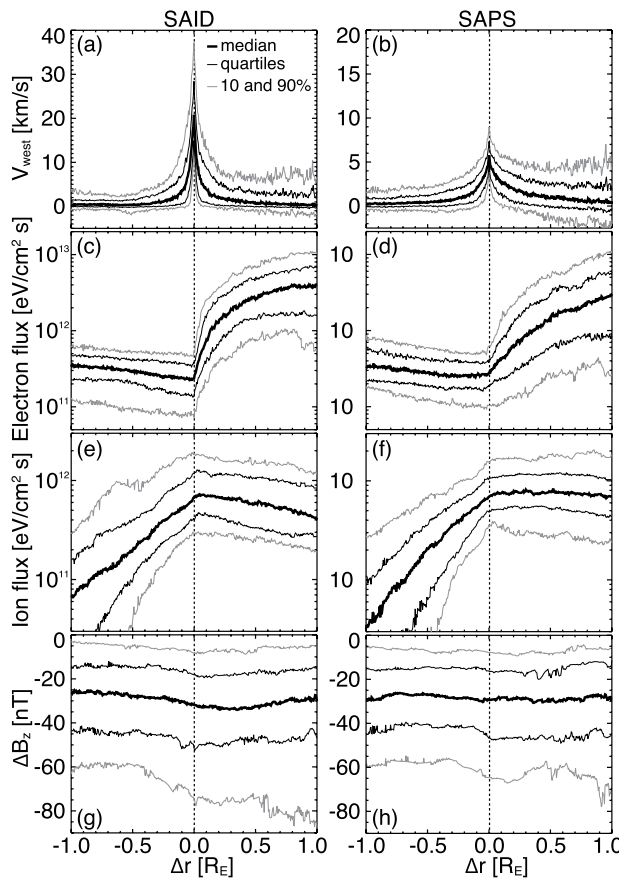


Figure 2. Superposed epoch analysis of (left) subauroral ion drifts (SAID) and (right) subauroral polarization streams (SAPS) events. (a and b) Westward velocity, (c and d) integrated energy flux of the plasma sheet electrons, (e and f) integrated energy flux of the ring current ions, and (g and h) ΔB_z . The epoch time is at the velocity peak.

both SAID and SAPS. The median ion flux for SAID and SAPS is almost the same, although the 90 and 75 percentiles of the ion flux for SAID are larger. These findings show that the ion flux is not necessarily larger for SAID, but the localized peak of the ion flux near the earthward boundary of the electron plasma sheet may be related to SAID.

Regarding current, ΔB_z for SAID is locally reduced at $\Delta r = -0.2\text{--}0.5 R_E$ (Figures 2g and 2h). The level of ΔB_z for SAID and SAPS is overall nearly the same, while a small number of events for SAID show substantial ΔB_z reduction (10 percentile). This behavior is consistent with the localization of the ring current ions for SAID and with the same peak level of the ion fluxes.

The westward velocity was converted to radially outward electric field by $E = -v \times B$, and the electric potential drop relative to the velocity peak was calculated as shown in Figures 3a and 3b. The median potential drop across SAID and SAPS is about the same (~ 4 kV). This indicates that SAID represent a state where the potential drop is more radially confined, even when the total potential drop across this region is the same as for SAPS. However, SAID events with large peak velocities have significantly larger potential drop ($\sim 10\text{--}20$ kV) than SAPS ($\sim 8\text{--}12$ kV). These numbers are somewhat smaller but comparable to those in earlier works (Foster & Vo, 2002; Landry & Anderson, 2018; Lejosne et al., 2018). The slight underestimation in our analysis is likely because we only integrate the potential drop within $1 R_E$ from the velocity peak, while SAPS can extend more than $1 R_E$ earthward.

Figures 3c and 3d compare the cold plasma density profiles in SAID and SAPS regions. At all five percentiles, the plasmapause for SAID is steeper (larger density gradient at $|\Delta r| < 0.1 R_E$) than that for SAPS. Both SAID and SAPS velocity peaks are statistically collocated with the plasmapause. SAID are mostly confined to the plasmapause, and Mishin and Puhl-Quinn (2007) interpreted that the association between SAID and a sharp plasmapause is due to a short-circuiting effect. However, a significant portion of the potential drop of SAID and much of the SAPS potential drop penetrate into the plasmasphere. We find that the plasmapause does not appear to fully short-circuit the SAPS/SAID electric field, but the inner edge of SAPS/SAID is more commonly related to the gradient of the ring current ion flux.

The wave electric and magnetic fields for SAID have a sharp peak at SAID except for the 10 and 25 percentiles for the wave magnetic field (Figures 3e and 3g). For SAPS, the wave electric field is much weaker (Figure 3h), and the wave magnetic field is nearly absent. The electrostatic waves outside SAID and SAPS are waves in the plasma sheet, and the electromagnetic waves earthward of SAID and SAPS are hiss and lower-hybrid waves that are often present in the plasmasphere.

To further investigate conditions of the SAID and SAPS events, we recorded properties of each event. Figures 4a and 4b show the locations of SAID and SAPS peak velocities on the X-Y plane. The dashed fan is the region of the event survey in this study. Results show that the occurrence regions of SAID and SAPS are similar to each other. The median radial distances are 4.9 (SAID) and 4.6 (SAPS) R_E , and the median local times are 21.6 (SAID) and 22.2 hr (SAPS). The peak velocity location does not have a clear dependence on the radial distance or local time.

Figure 4c shows the maximum electron and ion fluxes within $\pm 0.2 R_E$ from the velocity peak. In general, faster flow velocity tends to occur when the plasma sheet electron flux is higher. Most of the SAID events are found above $\sim 10^{12}$ [eV/cm² s] electron flux. In contrast, the flow velocity does not depend on the ring current ion flux. This result statistically supports earlier findings by Nishimura, Donovan, et al. (2020); Nishimura, Yang, et al. (2020) that SAID are closely related to larger electron injection to the pre-midnight inner magnetosphere.

Figure 4d is same as Figure 4c except that the data points are color-coded with radial potential drop across $\pm 1 R_E$ distance from the velocity peak. The potential drop increases with the ring current ion flux and has little

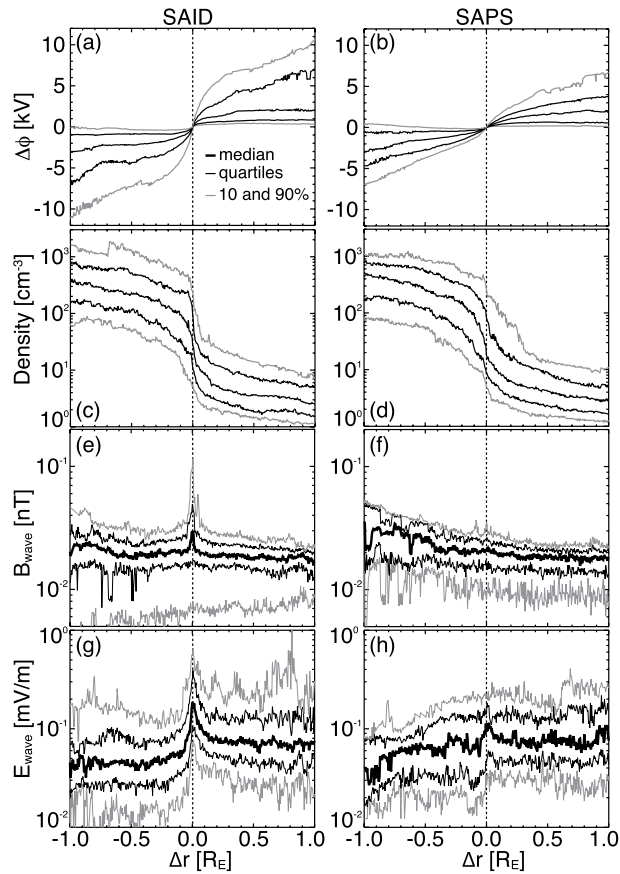


Figure 3. Same as Figure 2 but for (a and b) potential drop, (c and d) cold plasma density, (e and f) wave magnetic field, and (g and h) wave electric field.

correlation with the plasma sheet electron flux. The contrast between Figures 4c and 4d indicates that the peak velocity is related to the plasma sheet electron flux, while the total flow in the flow channel is related to the ring current ion flux. When the ion flux increases, the flow channel becomes wider and carry a larger amount of flow (larger potential drop), although the peak velocity does not necessarily increase with the ion flux.

We also recorded the median OMNI IMF, median *SYM-H*, and maximum *AE* over the 1-hr interval before each epoch time. The 1-hr interval ensures that these quantities represent preceding IMF and geomagnetic conditions without being influenced by IMF propagation time uncertainties or fluctuations. The IMF B_z is on average southward, but the peak velocity does not correlate with IMF B_z , and many of the intense SAID events occur at small IMF $|B_z|$ (Figure 4e). The SAID or SAPS events do not have a clear IMF B_y dependence (~ 0 median IMF B_y), although Gallardo-Lacourt et al. (2018) found a slight preference to negative IMF B_y for STEVE events, where intense SAID are expected.

The occurrence of SAID events is also not strongly correlated with *SYM-H* or *AE* (Figure 4f). *SYM-H* is mostly negative, but SAID can occur at small $|\text{SYM-}H|$ or *AE*. Figures 4e and 4f indicate that SAID do not require large storms and substorms but can occur in weakly disturbed conditions. We accordingly suggest that the SAID occurrence is not strongly controlled by large-scale driving conditions but are more closely related to the configuration of local plasma sheet electrons and ring current ions.

4. Conclusion

We performed a statistical study of SAPS and SAID in the inner magnetosphere. We found that SAID are commonly associated with higher plasma sheet electron fluxes just outside the velocity peak, with sharper radial gradient of the electron fluxes. We suggest that stronger electron injection to the pre-midnight inner magnetosphere is the

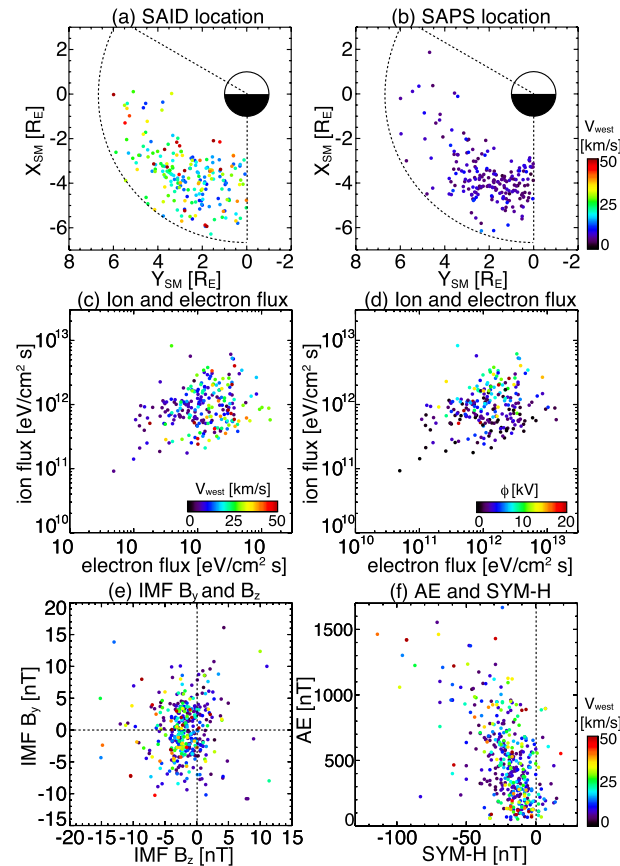


Figure 4. (a and b) Locations of the subauroral ion drifts (SAID) and subauroral polarization streams (SAPS) velocity peaks, (c and d) maximum electron and ion fluxes within $\pm 0.2 R_E$ from the velocity peak, (e) median IMF B_y and B_z for 1 hr before each epoch time, and (f) maximum AE and median $SYM-H$ indices for 1 hr before each epoch time. The colors are the peak velocity except for Panel (d) (potential drop).

primary condition for SAID. Ring current ions for SAID form a radial peak near SAID (also local ΔB_z depletion). Localized accumulation of ions near the earthward boundary of the plasma sheet electrons may be involved in SAID. However, median ring current ion fluxes for SAID and SAPS are essentially the same, and ring current strength for SAID is not necessarily larger than for SAPS.

The median potential drop across SAID and SAPS is nearly identical, but the potential drop for intense SAID is larger than that for SAPS. For SAID, the plasmapause is sharper and electromagnetic waves were stronger than for SAPS. Much of the potential drop is confined to the plasmapause, but a significant amount of the potential drop occurs in the plasmasphere. The earthward boundary of SAID and SAPS is closely related to ring current ion flux gradients.

The occurrence regions of SAID and SAPS do not have major statistical differences. SAID do not necessarily favor stronger geomagnetic activity. Ring current ion fluxes are not correlated strongly with the peak flow velocity, but rather correlated with the potential drop across the flow channel. We suggest that local plasma structures are more important for SAPS/SAID velocity features than global magnetospheric conditions. The dependence on local conditions raises a challenge of predicting SAPS/SAID velocity from solar wind and geomagnetic indices, and stresses importance of localized plasma transport for SAPS/SAID.

Although we identified a statistically significant relation between the electron flux and flow velocity, the correlation is not perfect. The present study did not investigate ionospheric effects due to difficulties in obtaining conductance data routinely and accurately. Ionospheric conditions should be considered in future studies to further advance understanding of SAPS/SAID in the inner magnetosphere.

Data Availability Statement

The THEMIS, RBSP and OMNI data were obtained through <http://themis.ssl.berkeley.edu/themisdata/> (daily CDF files of FGM/ESA/SST/EFI) and <https://cdaweb.gsfc.nasa.gov/pub/data/> (daily CDF files of RBSP EFW/EMFISIS/HOPE/MAGEIS, OMNI-1 min). Data processing used SPEDAS-V3.1 (Angelopoulos et al., 2019).

Acknowledgments

This work was supported by NASA Grant 80NSSC18K0657, 80NSSC20K0604, 80NSSC20K0725 and 80NSSC21K1321, NSF grant AGS-1907698 and AGS-2100975, and AFOSR grant FA9559-16-1-0364. THEMIS is supported by NASA NAS5-02099. We thank ISSI/ISSI-BJ for the “Multi-Scale Magnetosphere-Ionosphere-Thermosphere Interaction” and “Magnetotail Dipolarizations: Archimedes Force or Ideal Collapse?” workshops.

References

Ali, A. F., Malaspina, D. M., Elkington, S. R., Jaynes, A. N., Chan, A. A., Wygant, J., & Kletzing, C. A. (2016). Electric and magnetic radial diffusion coefficients using the Van Allen probes data. *Journal of Geophysical Research: Space Physics*, 121(10), 9586–9607. <https://doi.org/10.1002/2016JA023002>

Anderson, P. C., Carpenter, D. L., Tsuruda, K., Mukai, T., & Rich, F. J. (2001). Multisatellite observations of rapid subauroral ion drifts (SAID). *Journal of Geophysical Research*, 106(A12), 29585–29599. <https://doi.org/10.1029/2001JA000128>

Anderson, P. C., Hanson, W. B., Heelis, R. A., Craven, J. D., Baker, D. N., & Frank, L. A. (1993). A proposed production model of rapid subauroral ion drifts and their relationship to substorm evolution. *Journal of Geophysical Research*, 98(A4), 6069–6078. <https://doi.org/10.1029/92JA01975>

Anderson, P. C., Heelis, R. A., & Hanson, W. B. (1991). The ionospheric signatures of rapid subauroral ion drifts. *Journal of Geophysical Research*, 96(A4), 5785–5792. <https://doi.org/10.1029/90JA02651>

Angelopoulos, V., Cruce, P., Drozdov, A., Grimes, E. W., Hatzigeorgiu, N., King, D. A., et al. (2019). The Space physics environment data analysis system (SPEDAS). *Space Science Reviews*, 215(1), 9. <https://doi.org/10.1007/s11214-018-0576-4>

Foster, J. C., & Burke, W. J. (2002). Saps: A new categorization for sub-auroral electric fields. *Eos, Transactions American Geophysical Union*, 83(36), 393. <https://doi.org/10.1029/2002eo000289>

Foster, J. C., & Vo, H. B. (2002). Average characteristics and activity dependence of the subauroral polarization stream. *Journal of Geophysical Research*, 107(A12), 1475. <https://doi.org/10.1029/2002JA009409>

Gallardo-Lacourt, B., Nishimura, Y., Donovan, E., Gillies, D. M., Perry, G. W., Archer, W. E., et al. (2018). A statistical analysis of STEVE. *Journal of Geophysical Research: Space Physics*, 123(11), 9893–9905. <https://doi.org/10.1029/2018ja025368>

Galperin, Y. I. (2002). Polarization jet: Characteristics and a model. *Annales de Géophysique*, 20(3), 391–404. <https://doi.org/10.5194/angeo-20-391-2002>

He, F., Zhang, X.-X., & Chen, B. (2014). Solar cycle, seasonal, and diurnal variations of subauroral ion drifts: Statistical results. *Journal of Geophysical Research: Space Physics*, 119(6), 5076–5086. <https://doi.org/10.1002/2014JA019807>

He, F., Zhang, X.-X., Wang, W., & Chen, B. (2016). Double-peak subauroral ion drifts (DSAIDs). *Geophys. Research Letter*, 43(11), 5554–5562. <https://doi.org/10.1002/2016GL069133>

Karlsson, T., Marklund, G. T., Blomberg, L. G., & Mälkki, A. (1998). Subauroral electric fields observed by the Freja satellite: A statistical study. *Journal of Geophysical Research*, 103(A3), 4327–4341. <https://doi.org/10.1029/97JA00333>

Kurth, W. S., De Pascuale, S., Faden, J. B., Kletzing, C. A., Hospodarsky, G. B., Thaller, S., & Wygant, J. R. (2015). Electron densities inferred from plasma wave spectra obtained by the waves instrument on Van Allen Probes. *Journal of Geophysical Research: Space Physics*, 120(2), 904–914. <https://doi.org/10.1002/2014JA020857>

Landry, R. G., & Anderson, P. C. (2018). An Auroral boundary-oriented model of subauroral polarization streams (SAPS). *Journal of Geophysical Research: Space Physics*, 123(4), 3154–3169. <https://doi.org/10.1002/2017ja024921>

Lee, J. H., & Angelopoulos, V. (2014). On the presence and properties of cold ions near Earth's equatorial magnetosphere. *Journal of Geophysical Research: Space Physics*, 119(3), 1749–1770. <https://doi.org/10.1002/2013JA019305>

Lejosne, S., Kunduri, B. S. R., Mozer, F. S., & Turner, D. L. (2018). Energetic electron injections deep into the inner magnetosphere: A result of the subauroral polarization stream (SAPS) potential drop. *Geophysical Research Letters*, 45(9), 3811–3819. <https://doi.org/10.1029/2018gl077969>

Lejosne, S., & Mozer, F. S. (2017). Subauroral Polarization Streams (SAPS) duration as determined from Van Allen probe successive electric drift measurements. *Geophysical Research Letters*, 44(18), 9134–9141. <https://doi.org/10.1002/2017gl074985>

MacDonald, E. A., Donovan, E. F., Nishimura, Y., Case, N. A., Gillies, D. M., Gallardo-Lacourt, B., et al. (2018). New science in plain sight: Citizen scientists lead to discovery of optical structure in the upper atmosphere. *Science Advances*, 3, eaao0030. <https://doi.org/10.1126/sciadv.aao0030>

Mishin, E. V., & Puhl-Quinn, P. A. (2007). SAID: Plasmaspheric short circuit of substorm injections. *Geophysical Research Letters*, 34(24), L24101. <https://doi.org/10.1029/2007GL031925>

Mishin, E. V., Puhl-Quinn, P. A., & Santolik, O. (2010). SAID: A turbulent plasmaspheric boundary layer. *Geophysical Research Letters*, 37(7), L07106. <https://doi.org/10.1029/2010GL042929>

Nishimura, Y., Artemyev, A. V., Lyons, L. R., Gabrielse, C., Donovan, E. F., & Angelopoulos, V. (2022). Space-ground observations of dynamics of substorm onset beads. *Journal of Geophysical Research: Space Physics*, 127(2), e2021JA030004. <https://doi.org/10.1029/2021ja030004>

Nishimura, Y., Bortnik, J., Li, W., Thorne, R. M., Ni, B., Lyons, L. R., et al. (2013). Structures of dayside whistler-mode waves deduced from conjugate diffuse aurora. *Journal of Geophysical Research: Space Physics*, 118(2), 664–673. <https://doi.org/10.1029/2012JA018242>

Nishimura, Y., Donovan, E. F., Angelopoulos, V., & Nishitani, N. (2020). Dynamics of auroral precipitation boundaries associated with STEVE and SAID. *Journal of Geophysical Research: Space Physics*, 125(8), e2020JA028067. <https://doi.org/10.1029/2020ja028067>

Nishimura, Y., Gallardo-Lacourt, B., Zou, Y., Mishin, E., Knudsen, D. J., Donovan, E. F., et al. (2019). Magnetospheric signatures of STEVE: Implications for the magnetospheric energy source and interhemispheric conjugacy. *Geophysical Research Letters*, 46(11), 5637–5644. <https://doi.org/10.1029/2019gl082460>

Nishimura, Y., Shinbori, A., Ono, T., Iizima, M., & Kumamoto, A. (2006). Storm-time electric field distribution in the inner magnetosphere. *Geophysical Research Letters*, 33(22), L22102. <https://doi.org/10.1029/2006GL027510>

Nishimura, Y., Wygant, J., Ono, T., Iizima, M., Kumamoto, A., Brautigam, D., & Friedel, R. (2008). SAPS measurements around the magnetic equator by CRRES. *Geophysical Research Letters*, 35(10), L10104. <https://doi.org/10.1029/2008GL033970>

Nishimura, Y., Yang, J., Weygand, J. M., Wang, W., Kosar, B., Donovan, E. F., et al. (2020). Magnetospheric conditions for STEVE and SAID: Particle injection, substorm surge, and field-aligned currents. *Journal of Geophysical Research: Space Physics*, 125(8), e2020JA027782. <https://doi.org/10.1029/2020ja027782>

Thaller, S. A., Wygant, J. R., Dai, L., Breneman, A. W., Kersten, K., Cattell, C. A., et al. (2015). Van Allen Probes investigation of the large-scale duskward electric field and its role in ring current formation and plasmasphere erosion in the 1 June 2013 storm. *Journal of Geophysical Research: Space Physics*, 120(6), 4531–4543. <https://doi.org/10.1002/2014ja020875>

Tsyganenko, N. A. (2002). A model of the near magnetosphere with a dawn-dusk asymmetry, 2. Parameterization and fitting to observations. *Journal of Geophysical Research*, 107(A8). <https://doi.org/10.1029/2001JA000220>

Wang, H., Ridley, A. J., Lühr, H., Liemohn, M. W., & Ma, S. Y. (2008). Statistical study of the subauroral polarization stream: Its dependence on the cross-polar cap potential and subauroral conductance. *Journal of Geophysical Research*, 113(A12), A12311. <https://doi.org/10.1029/2008JA013529>

Yeh, H.-C., Foster, J. C., Rich, F. J., & Swider, W. (1991). Storm time electric field penetration observed at mid-latitude. *Journal of Geophysical Research*, 96(A4), 5707–5721. <https://doi.org/10.1029/90JA02751>